sensors

MDPI

Article

Resilient Adaptive Event-Triggered Load Frequency Control of Network-Based Power Systems against Deception Attacks

Xiao Zhang, Fan Yang * and Xiang Sun

College of Mechanical & Electronic Engineering, Nanjing Forestry University, Nanjing 210037, China; ZhX1@njfu.edu.cn (X.Z.); sx032812@njfu.edu.cn (X.S.)
* Correspondence: yfan0510@njfu.edu.cn

Abstract: This paper investigates the problem of networked load frequency control (LFC) of power systems (PSs) against deception attacks. To lighten the load of the communication network, a new adaptive event-triggered scheme (ETS) is developed on the premise of maintaining a certain control performance of LFC systems. Compared with the existing ETSs, the proposed adaptive ETS can adjust the number of triggering packets, along with the state changes in the presence of deception attacks, which can reduce the average data-releasing rate. In addition, sufficient conditions can be derived, providing a trade-off between the limited network communication resources and the desired control performance of PSs. Finally, an application case is presented for the PSs to demonstrate the advantages of the proposed approach.

Keywords: load frequency control (LFC); deception attacks; adaptive event-triggered scheme (ETS); power systems (PSs)

Citation: Zhang, X.; Yang, F.; Sun, X. Resilient Adaptive Event-Triggered Load Frequency Control of Network-Based Power Systems against Deception Attacks. *Sensors* **2021**, *21*, 7047. https://doi.org/10.3390/s21217047

Academic Editor: Yang Yue

Received: 28 August 2021
Accepted: 20 October 2021
Published: 24 October 2021

1. Introduction

It is known that load frequency control (LFC) is a core component of PSs, which governs the system frequency and power exchange between regions in an optimally scheduled way [1–3]. Proportional-integral (PI) control has been widely utilized as a common control strategy in LFC [4–6]. For example, the authors in [6] studied the area LFC problem using fuzzy gain scheduling with a PI controller. With the development of the PSs, control signals are transmitted via a special power channel and an networked communication infrastructure, which brings new challenges to the PI controller design of LFC. Recently, a lot of the published literature [7–11] has concerned networked LFC. For instance, in [8], an active interference suppression control method was proposed for interconnected LFC systems.

Since the control signals of PSs are transmitted through the communication network, the potential risks of LFC systems increases, such as cyber attacks [12–17]. Cyber-attacks have receieved great attention in recent years [1,2]. Usually, cyber-attacks discussed in the literature include denial of service (DoS) attacks and deception attacks. The deception attackers launch a attack by destroying data integrity, such as tampering or replacing transmitted data. In [18], a new control method was proposed in distributed networks subject to deception attacks. The DoS attacks prevent data transmission by occupying the shared network channel, thereby degrading the system performance. A resilient ETS was well-designed in [19] for LFC systems under DoS attacks. In [14], the event-triggered control was studied for multi-agent systems under DoS attacks.

In NCS, the time-triggered scheme (TTS) is widely used to obtain the system information through the sampler, under which a fixed sampling interval can guarantee the desired performance even if there are uncertainties, time-delays, external disturbances, etc. [20,21]. However, too many "unnecessary" sampling signals are transmitted via the network, which leads to a waste of resources [22,23]. To deal with these shortcomings, an event-triggered scheme (ETS) has been widely applied to ease the network burden in recent

decades. Compared to the TTS, the sampling data packets are released only when an event generated by some elaborate condition occurs, which can effectively improve resource utilization while ensuring a satisfied system performance [24–27]. However, due to the complexity of the system and the contradiction between better system performance and a lower data transmission rate, it is usually difficult to design the threshold of event-triggered conditions in the practical application system. Therefore, some state-of-the-art ETSs have been proposed, such as memory-based ETS and adaptive ETS. The authors in [28] proposed a memory-based ETS for T-S fuzzy systems, wherein some historical triggered data were utilized in the ETS so that the control performance can be ensured. The authors in [29,30] proposed an adaptive ETS for nonlinear systems, wherein the threshold can be adjusted with the system states. However, the problem of H_∞-based LFC for network-based PSs under deception attacks by adopting adaptive ETS has not yet been reported, which prompted this study.

In sum, the goal of this work is to design an adaptive event-triggered controller for LFC systems subject to deception attacks. Differing from the existing ETS with a preset threshold, the improved adaptive ETS can adjust the number of triggering packets along with the state changes, under which the transmission rate can be cut down while maintaining the desired frequency performance of LFC systems under deception attacks.

2. Problem Formulation

Figure 1 displays a block diagram of a single-area LFC power system, where the area control error is presumed to be transmitted to the PI controller via a shared communication network.

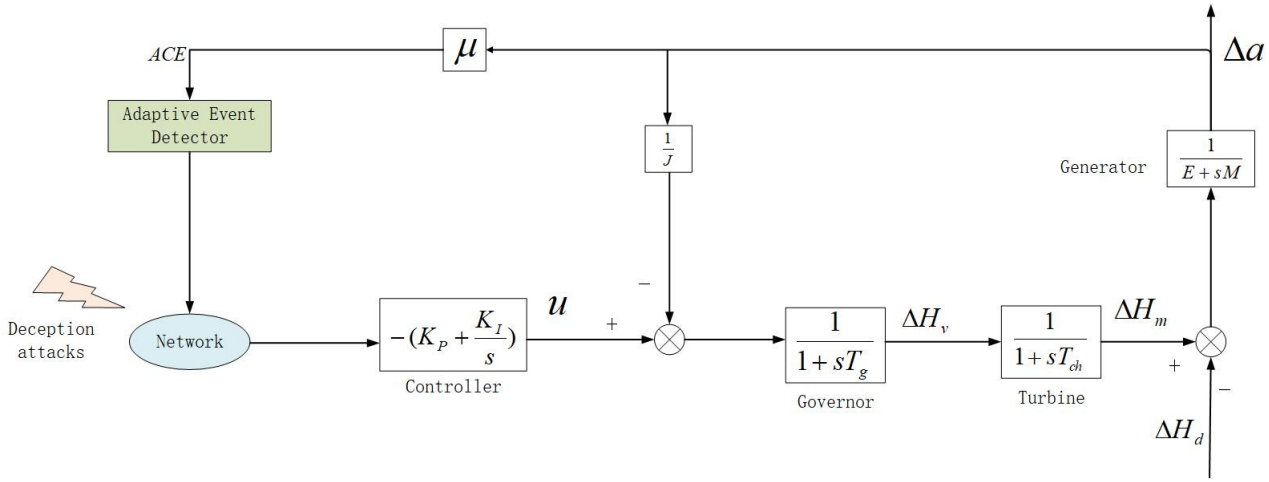

Figure 1. Structure of the LFC system with adaptive ETS.

2.1. Description of the LFC Systems

As shown in Figure 1, the model of the LFC systems can be indicated as follows [31]

$$\begin{cases} \Delta a(s) = \frac{1}{s\mathcal{M}+\mathcal{E}}(\Delta\mathcal{H}_m(s) - \Delta\mathcal{H}_d(s)), \\ \Delta\mathcal{H}_m(s) = \frac{1}{1+s\mathcal{T}_{ch}}\Delta\mathcal{H}_v(s), \\ \Delta\mathcal{H}_v(s) = \frac{1}{1+s\mathcal{T}_g}\left(u(s) - \frac{1}{\mathcal{J}}\Delta a(s)\right), \\ \mathcal{ACE}(s) = \mu\Delta a(s), \end{cases} \tag{1}$$

where the symbols of the LFC system are listed in Table 1 [2].

By applying the inverse Laplace transform to (1), it can be obtained that

$$\begin{cases} \Delta\dot{a}(t) = \frac{1}{\mathcal{M}}(\Delta\mathcal{H}_m(t) - \Delta\mathcal{H}_d(t) - \mathcal{E}\Delta a(t)), \\ \Delta\dot{\mathcal{H}}_m(t) = \frac{1}{\mathcal{T}_{ch}}(\Delta\mathcal{H}_v(t) - \Delta\mathcal{H}_m(t)), \\ \Delta\dot{\mathcal{H}}_v(t) = \frac{1}{\mathcal{T}_g}\Big(u(t) - \frac{1}{\mathcal{J}}\Delta a(t) - \Delta\mathcal{H}_v(t)\Big). \end{cases} \tag{2}$$

Table 1. Meanings of the symbols for the LFC system.

Symbol	Meaning
$\mathcal{T}_g$	Time constant of governor
$\Delta\mathcal{H}_m(s)$	Mechanical output of the generator
$\Delta\mathcal{H}_d(s)$	External interference
$u(s)$	Control output
$\mathcal{ACE}(s)$	Area control error
$\mathcal{E}$	Generator damping coefficient
$\mathcal{M}$	Moment of inertia of the generator
$\Delta a(s)$	Frequency deviation
μ	Frequency bias factor
$\mathcal{J}$	Speed drop
$\mathcal{T}_{ch}$	Time constant of turbine
$\Delta\mathcal{H}_v(s)$	Position deviation of the valve

Similar to [10], we can obtain the state-space representation for LFC systems, as follows

$$\begin{cases} \dot{\hat{x}}(t) = \mathbb{A}\hat{x}(t) + \mathbb{B}u(t) + \mathbb{F}\omega(t), \\ \hat{y}(t) = \mathbb{C}\hat{x}(t), \end{cases} \tag{3}$$

where $\hat{x}(t) = [\Delta a(t) \ \ \Delta\mathcal{H}_m(t) \ \ \Delta\mathcal{H}_v(t)]^T$, $\omega(t) = \Delta\mathcal{H}_d(t)$, $\hat{y}(t) = \mathcal{ACE}(t)$, and

$$\mathbb{A} = \begin{bmatrix} -\frac{\mathcal{E}}{\mathcal{M}} & \frac{1}{\mathcal{M}} & 0 \\ 0 & -\frac{1}{\mathcal{T}_{ch}} & \frac{1}{\mathcal{T}_{ch}} \\ -\frac{1}{\mathcal{J}\mathcal{T}_g} & 0 & -\frac{1}{\mathcal{T}_g} \end{bmatrix}, \mathbb{B} = [0 \ \ 0 \ \ \frac{1}{\mathcal{T}_g}]^T, \mathbb{C} = \begin{bmatrix} \mu & 0 & 0 \end{bmatrix}, \mathbb{F} = [-\frac{1}{\mathcal{M}} \ \ 0 \ \ 0]^T.$$

2.2. Adaptive ETS Controller Design

Simular to [10], the PI control strategy of the LFC systems is designed as

$$u(t) = -\mathcal{K}_P\mathcal{ACE}(t) - \mathcal{K}_I\int_0^t \mathcal{ACE}(s)ds, \tag{4}$$

where $\mathcal{K}_P$ denotes proportional gain and $\mathcal{K}_I$ stands for integral gain.

For convenience of obtaining the controller gains, we transform the above PI control form into the output feedback problem. Then, we redefine the output variables

$$y(t) = [\mathcal{ACE}(t) \ \ \int_0^t \mathcal{ACE}(s)ds]^T.$$

Define $\mathcal{K} = [\mathcal{K}_P \ \ \mathcal{K}_I]$, and we can rewrite (4) as

$$u(t) = -\mathcal{K}y(t). \tag{5}$$

However, the sampled signal of $\mathcal{ACE}(t)$ of networked LFC systems will only be released to the PI controller via the network when the preset condition is satisfied [20]. To adjust the number of triggering packets in the LFC system, along with the state changes under deception attacks, an improved adaptive ETS is put forward, as follows:

$$t_{k+1}h = t_k h + \min_{l\in\mathbb{N}}\{lh|\varkappa^T(i_l h)\phi\varkappa(i_l h) > \sigma(t)x^T(t_k h)\phi x(t_k h)\}, \tag{6}$$

where h is the sampling period, ϕ is a positive symmetric matrix to be designed, $t_k h$ is the data-releasing instant, $\varkappa(i_l h) = y(i_l h) - y(t_k h)$, $i_l h = lh + t_k h, l \in N, i_l h \in (t_k h, t_{k+1}h]$, $\{t_0, t_1, t_2, \dots\} \subset \{0, 1, 2, \dots\}$, and

$$\sigma(t) = \alpha\left(1 - \frac{2}{\pi}\arctan(\iota\|y(i_l h)\|)\right), \tag{7}$$

wherein $\alpha \in (0, 1)$ is the upper bound of $\sigma(t)$, ι and α are given positive constants.

Remark 1. *It can be seen from (7) that $\sigma(t)$ can adaptively adjusted to the system states by a arctangent function, which is different from the existing ETS with a constant threshold. When the system states fluctuate, $\sigma(t)$ will be adaptively adjusted to a lower value, by which more packets with the system information can be released to the controller. When the system is stable, $\sigma(t)$ will be automatically adjusted to a larger value to decrease the release rate of sampled packets.*

Based on the condition (6), one can obtain that

$$y(t_k h) = y(i_l h) - \varkappa(i_l h). \tag{8}$$

Since the communication network is vulnerable to cyber attacks, the transmission signal can be written as

$$\hat{y}(t) = \varphi(t)\eth(t) + (1 - \varphi(t))y(t_k h), \tag{9}$$

where the Bernoulli variable $\varphi(t) \in \{0, 1\}$ is introduced to characterize the behavior of random deception attacks, $\mathbb{E}\{\varphi(t)\} = \bar{\varphi}$, $\mathbb{E}\{(\varphi(t) - \bar{\varphi})^2\} = \rho^2$ and the nonlinear attack signal $\eth(t)$ satisfies

$$\|\eth(t)\|^2 \leq \|\mathcal{G}y(t)\|^2, \tag{10}$$

where $\mathcal{G}$ is a known matrix with appropriate dimension.

Remark 2. *Cyber-attack has receieved great attention in recent years since it is one of the major threats to system stability [1,2,19]. Usually, cyber-attacks discussed in the literature include DoS attacks and deception attacks. The DoS attacks prevent data transmission by occupying the shared network channel, thereby degrading system performance. The deception attackers launch an attack by destroying data integrity, such as tampering with or replacing transmitted data. In this paper, we consider a kind of deception attack when investigating the LFC problem of PSs.*

Remark 3. *When $\varphi(t) = 1$, the true measurement data are replaced with the data of deception attacks. Otherwise, the true measurement data can be transmitted to the controller.*

Considering the deception attacks, the output of the controller in (5) can be rewritten as

$$u(t) = -\mathcal{K}\hat{y}(t). \tag{11}$$

2.3. Closed-Loop Control of LFC Systems

According to the adaptive ETS in (6), the current signal is maintained by the zero-order holder (ZOH) until the next packet is transmitted. Therefore, we need to divide the interval $\Pi = [\bar{m}\ ,\ \bar{n})$ into $\wp + 1$ pieces, where $\bar{m} = t_k h + \lambda_{t_k}$, $\bar{n} = t_{k+1}h + \lambda_{t_{k+1}}$. The network-induced delay at instant $t_k h$ is denoted by λ_{t_k} and the holding interval Π can be divided into

$$\Pi = \cup_{l=0}^{\wp}\Pi_l, \tag{12}$$

where

$$\Pi_l = [t_k h + lh + \vartheta, t_{k+1} h + (l+1)h + \vartheta),$$
$$\vartheta = \begin{cases} \lambda_{t_k}, & l = 0, 1, \ldots, \wp - 1, \\ \lambda_{t_{k+1}}, & l = \wp, \end{cases}$$
$$\wp + 1 = t_{k+1} - t_k.$$

Define

$$\lambda(t) = t - i_l h,$$

where $i_l h = t_k h + lh$, $0 \leq \lambda_{t_k} \leq \lambda(t) \leq \lambda_M = \bar{\lambda}$, $\lambda_M = h + \max\{\lambda_{t_k}\}$. Then, $\hat{y}(t)$ can be represented by

$$\hat{y}(t) = \varphi(t)\eth(t) + (1 - \varphi(t)(y(t - \lambda(t)) - \varkappa(t - \lambda(t))), \tag{13}$$

for $t \in \Pi_l$.

Redefining new variables $x(t) = [\Delta a(t) \;\; \Delta\mathcal{H}_m(t) \;\; \Delta\mathcal{H}_v(t) \;\; \int_0^t \mathcal{ACE}(s)ds]^T$. Combine (4)–(13), the LFC systems (3) with an adaptive event-triggered PI controller against deception attacks can be formulated as

$$\begin{cases} \dot{x}(t) = \mathcal{A}x(t) - (1 - \varphi(t))\mathcal{BKC}x(t - \lambda(t)) + (1 - \varphi(t))\mathcal{BK}\varkappa(t - \lambda(t)) + \mathcal{F}\omega(t) \\ \qquad\quad - \mathcal{BK}\varphi(t)\eth(t), \\ y(t) = \mathcal{C}x(t), t \in \Pi_l. \end{cases} \tag{14}$$

where

$$\mathcal{A} = \begin{bmatrix} -\frac{\mathcal{E}}{\mathcal{M}} & \frac{1}{\mathcal{M}} & 0 & 0 \\ 0 & -\frac{1}{\mathcal{T}_{ch}} & \frac{1}{\mathcal{T}_{ch}} & 0 \\ -\frac{1}{\mathcal{R}\mathcal{T}_g} & 0 & -\frac{1}{\mathcal{T}_g} & 0 \\ \mu & 0 & 0 & 0 \end{bmatrix}, \mathcal{B} = \begin{bmatrix} 0 \\ 0 \\ \frac{1}{\mathcal{T}_g} \\ 0 \end{bmatrix}, \mathcal{C} = \begin{bmatrix} \mu & 0 & 0 & 0 \\ 0 & 0 & 0 & 1 \end{bmatrix}, \mathcal{F} = \begin{bmatrix} -\frac{1}{\mathcal{M}} \\ 0 \\ 0 \\ 0 \end{bmatrix}.$$

The purpose of this article is to design the adaptive event-triggered PI controller subject to deception attacks, while ensuring that $\mathbb{E}\{\|y(t)\|\} \leq \mathbb{E}\{\gamma\|\omega(t)\|\}$ holds with zero initial state conditions when $\omega(t) \neq 0$, and the LFC system (14) could achieve stability with $\omega(t) = 0$.

3. Main Results

In this section, we use the Lyapunov–Krasovskii function method to derive the stability criteria of the LFC system. Then, the weight matrix of adaptive ETS and the controller gain will be calculated by LMIs. The statement of sufficient conditions for the LFC system are shown in the following.

Theorem 1. *For given scalars $\bar{\lambda} > 0$, $\alpha \in (0, 1)$, $\bar{\varphi} \in (0, 1)$, ρ, H_∞ norm bound γ, and matrix $\mathcal{K}$, the system (14) is asymptotically stable, if there exist matrices $\mathcal{P} > 0, \mathcal{P}_2 > 0, \mathcal{R} > 0, \mathcal{Q} > 0$ $\mathcal{W} > 0$ and a matrix $\mathcal{U}$ such that*

$$\begin{bmatrix} \mathcal{R} & * \\ \mathcal{U} & \mathcal{R} \end{bmatrix} > 0, \tag{15}$$

$$\Xi = \begin{bmatrix} \Xi_{11} & * & * & * \\ \Xi_{21} & -\bar{\varphi}P_2 & * & * \\ \Xi_{31} & \Xi_{32} & -(\mathcal{R} + \mathcal{W}) & * \\ \Xi_{41} & \Xi_{42} & 0 & -(\mathcal{R} + \mathcal{W}) \end{bmatrix} < 0, \tag{16}$$

where

$$\Xi_{11}=\begin{bmatrix}\Psi_{11} & * & * & * & *\\ \Psi_{21} & \Psi_{22} & * & * & *\\ \mathcal{U} & \mathcal{R}-\mathcal{U} & -\mathcal{Q}-\mathcal{R} & * & *\\ (1-\bar{\varphi})\mathcal{K}^T\mathcal{B}^T\mathcal{P} & -\alpha\phi\mathcal{C} & 0 & -\phi+\alpha\phi & *\\ \mathcal{F}^T\mathcal{P} & 0 & 0 & 0 & -\gamma^2 I\end{bmatrix},$$

$$\begin{aligned}
\Psi_{11}=&\mathcal{A}^T\mathcal{P}+\mathcal{P}\mathcal{A}+\mathcal{Q}-\mathcal{R}-\frac{\pi^2}{4}\mathcal{W}+\mathcal{C}^T\mathcal{C}+\bar{\varphi}\mathcal{C}^T\mathcal{G}^T\mathcal{P}_2\mathcal{G}\mathcal{C},\\
\Psi_{21}=&(\bar{\varphi}-1)\mathcal{C}^T\mathcal{K}^T\mathcal{B}^T\mathcal{P}+\mathcal{R}-\mathcal{U}+\frac{\pi^2}{4}\mathcal{W},\\
\Psi_{22}=&\mathcal{U}+\mathcal{U}^T-2\mathcal{R}-\frac{\pi^2}{4}\mathcal{W}+\alpha\mathcal{C}^T\phi\mathcal{C},\\
\Xi_{21}=&[-\bar{\varphi}\mathcal{K}^T\mathcal{B}^T\mathcal{P}\ \ 0\ \ 0\ \ 0\ \ 0],\\
\Xi_{31}=&\bar{\lambda}(\mathcal{R}+\mathcal{W})\mathrm{Y}_1,\\
\Xi_{32}=&-\bar{\lambda}\bar{\varphi}(\mathcal{R}+\mathcal{W})\mathcal{B}\mathcal{K},\\
\Xi_{41}=&\bar{\lambda}\rho(\mathcal{R}+\mathcal{W})\mathrm{Y}_2,\\
\Xi_{42}=&\bar{\lambda}\rho(\mathcal{R}+\mathcal{W})\mathcal{B}\mathcal{K},\\
\mathrm{Y}_1=&\begin{bmatrix}\mathcal{A} & (\bar{\varphi}-1)\mathcal{B}\mathcal{K}\mathcal{C} & 0 & (1-\bar{\varphi})\mathcal{B}\mathcal{K} & \mathcal{F}\end{bmatrix},\\
\mathrm{Y}_2=&\begin{bmatrix}0 & -\mathcal{B}\mathcal{K}\mathcal{C} & 0 & \mathcal{B}\mathcal{K} & 0\end{bmatrix}.
\end{aligned}$$

Proof. Construct a Lyapunov–Krasovskii function in [31] for the system (14) as

$$\begin{aligned}
V(t)=&x^T(t)\mathcal{P}x(t)+\int_{t-\bar{\lambda}}^{t}x^T(s)\mathcal{Q}x(s)ds+\bar{\lambda}\int_{t-\bar{\lambda}}^{t}\int_{s}^{t}\dot{x}^T(v)\mathcal{R}\dot{x}(v)dvds\\
&+\bar{\lambda}^2\int_{i_lh}^{t}\dot{x}^T(s)\mathcal{W}\dot{x}(s)ds-\frac{\pi^2}{4}\int_{i_lh}^{t}[x(s)-x(i_lh)]^T\mathcal{W}[x(s)-x(i_lh)]ds.
\end{aligned}\tag{17}$$

Define $\mathcal{F}(t)=\bar{\lambda}^2\dot{x}^T(t)\mathcal{R}\dot{x}(t)+\bar{\lambda}^2\dot{x}^T(t)\mathcal{W}\dot{x}(t)$; then, the following results can be derived from (17),

$$\begin{aligned}
\mathbb{E}\{\dot{V}(t)\}=&2x^T(t)\mathcal{P}\Lambda_1(t)+x^T(t)\mathcal{Q}x(t)-x^T(t-\bar{\lambda})\mathcal{Q}x(t-\bar{\lambda})-\bar{\lambda}\int_{t-\bar{\lambda}}^{t}\dot{x}^T(s)\mathcal{R}\dot{x}(s)ds\\
&-\frac{\pi^2}{4}[x(t)-x(i_lh)]^T\mathcal{W}[x(t)-x(i_lh)]+\mathbb{E}\{\mathcal{F}(t)\},
\end{aligned}\tag{18}$$

where

$$\begin{aligned}
&\mathbb{E}\{\mathcal{F}(t)\}=\bar{\lambda}^2\Lambda_1^T(t)(\mathcal{R}+\mathcal{W})\Lambda_1(t)+\bar{\lambda}^2\rho^2\Lambda_2^T(t)(\mathcal{R}+\mathcal{W})\Lambda_2(t),\\
&\Lambda_1(t)=\mathcal{A}x(t)-(1-\bar{\varphi})\mathcal{B}\mathcal{K}\mathcal{C}x(t-\lambda(t))+(1-\bar{\varphi})\mathcal{B}\mathcal{K}\varkappa(t-\lambda(t))+\mathcal{F}\omega(t)-\bar{\varphi}\mathcal{B}\mathcal{K}\eth(t),\\
&\Lambda_2(t)=\mathcal{B}\mathcal{K}\varkappa(t-\lambda(t))-\mathcal{B}\mathcal{K}\mathcal{C}x(t-\lambda(t))+\mathcal{B}\mathcal{K}\eth(t).
\end{aligned}$$

From the adaptive ETS (6), one can obtain

$$\sigma(t)[y(i_lh)-\varkappa(i_lh)]^T\phi[y(i_lh)-\varkappa(i_lh)]-\varkappa(i_lh)^T\phi\varkappa(i_lh)\geq 0.\tag{19}$$

According to inequality (10), it has

$$\bar{\varphi}y^T(t)\mathcal{G}^T\mathcal{P}_2\mathcal{G}y(t)-\bar{\varphi}\eth^T(t)\mathcal{P}_2\eth(t)\geq 0,\tag{20}$$

where $\mathcal{P}_2$ is a positive symmetric matrix.

Define $\Omega(t) = \gamma^2\omega^T(t)\omega(t) - y^T(t)y(t)$; then, combining (15)–(20), and using Schur complement lemma and the method in [31] follows:

$$\mathbb{E}\{\dot{V}(t)\} \leq \mathbb{E}\{\Psi^T(t)\Xi\Psi(t)\} + \mathbb{E}\{\Omega(t)\}, \tag{21}$$

where

$$\Psi^T(t) = [x^T(t)\ \ x^T(t-\lambda(t))\ \ x^T(t-\bar{\lambda})\ \ \varkappa^T(t-\lambda(t))\ \ \omega^T(t)\ \ \eth^T(t)].$$

According to (15) and (16), we can conclude that $\mathbb{E}\{\Psi^T(t)\Xi\Psi(t)\} \leq 0$, which means that

$$\mathbb{E}\{\dot{V}(t)\} < \mathbb{E}\{\Omega(t)\}. \tag{22}$$

Taking the integration on both sides for (22) from 0 to $+\infty$, we have

$$\mathbb{E}\{V(+\infty) - V(0)\} < \mathbb{E}\{\int_0^{+\infty}\Omega(t)dt\}. \tag{23}$$

The LFC systems (14) are asymptotically stable with zero initial conditions when $\omega(t) = 0$, and $\mathbb{E}\{\|y(t)\|\} \leq \mathbb{E}\{\gamma\|\omega(t)\|\}$ when $\omega(t) \neq 0$. The proof is complete. □

Theorem 2. *For given scalars $\bar{\lambda} > 0$, $\alpha \in (0,1)$, $\bar{\varphi} \in (0,1)$, ρ, H_∞ norm bound γ, the system (14) is asymptotically stable, if there are symmetric and positive definite matrices $\mathcal{L}$, $\mathcal{X}$, $\tilde{\mathcal{Q}}$, $\tilde{\mathcal{W}}$, $\tilde{\mathcal{R}}$, matrices $\tilde{\mathcal{U}}$ and $\mathcal{N}$ with appropriate dimensions, such that the following linear matrix inequalities hold:*

$$\mathcal{C}\mathcal{X} = \mathcal{L}\mathcal{C}, \tag{24}$$

$$\begin{bmatrix} \tilde{\mathcal{R}} & * \\ \tilde{\mathcal{U}} & \tilde{\mathcal{R}} \end{bmatrix} > 0, \tag{25}$$

$$\tilde{\Xi} = \begin{bmatrix} \tilde{\Theta}_{11} & * & * \\ \tilde{\Theta}_{21} & \tilde{\Theta}_{22} & * \\ \tilde{\Theta}_{31} & 0 & \tilde{\Theta}_{33} \end{bmatrix} < 0, \tag{26}$$

where

$$\tilde{\Theta}_{11} = \begin{bmatrix} \tilde{\Xi}_{11} & * & * & * & * & * \\ \tilde{\Xi}_{21} & \tilde{\Xi}_{22} & * & * & * & * \\ \tilde{\mathcal{U}} & \tilde{\mathcal{R}} - \tilde{\mathcal{U}} & -\tilde{\mathcal{Q}} - \tilde{\mathcal{R}} & * & * & * \\ (1-\bar{\varphi})\mathcal{N}^T\mathcal{B}^T & -\alpha\tilde{\phi}\mathcal{C} & 0 & -\tilde{\phi} + \alpha\tilde{\phi} & * & * \\ \tilde{\Xi}_{51} & 0 & 0 & 0 & -\gamma^2 I & * \\ -\bar{\varphi}\mathcal{N}^T\mathcal{B}^T & 0 & 0 & 0 & 0 & -\bar{\varphi}\mathcal{L} \end{bmatrix},$$

$$\tilde{\Xi}_{11} = \mathcal{X}\mathcal{A}^T + \mathcal{A}\mathcal{X} + \tilde{\mathcal{Q}} - \tilde{\mathcal{R}} - \frac{\pi^2}{4}\tilde{\mathcal{W}},$$

$$\tilde{\Xi}_{21} = (\bar{\varphi} - 1)\mathcal{C}^T\mathcal{N}^T\mathcal{B}^T + \tilde{\mathcal{R}} - \tilde{\mathcal{U}} + \frac{\pi^2}{4}\tilde{\mathcal{W}},$$

$$\tilde{\Xi}_{22} = -2\tilde{\mathcal{R}} + \tilde{\mathcal{U}} + \tilde{\mathcal{U}}^T - \frac{\pi^2}{4}\tilde{\mathcal{W}} + \alpha\mathcal{C}^T\tilde{\phi}\mathcal{C}, \tilde{\Xi}_{51} = \mathcal{F}^T,$$

$$\tilde{\Theta}_{21} = \begin{bmatrix} \bar{\lambda}\mathcal{A}\mathcal{X} & -\bar{\lambda}(1-\bar{\varphi})\mathcal{B}\mathcal{N}\mathcal{C} & 0 & \bar{\lambda}(1-\bar{\varphi})\mathcal{B}\mathcal{N} & \bar{\lambda}\mathcal{F} & -\bar{\lambda}\bar{\varphi}\mathcal{B}\mathcal{N} \\ 0 & -\bar{\lambda}\rho\mathcal{B}\mathcal{N}\mathcal{C} & 0 & \bar{\lambda}\rho\mathcal{B}\mathcal{N} & 0 & \bar{\lambda}\rho\mathcal{B}\mathcal{N} \end{bmatrix},$$

$$\tilde{\Theta}_{22} = diag\Big\{-2\zeta_0\mathcal{X} + \zeta_0^2(\mathcal{R} + \mathcal{W}),\ -2\zeta_1\mathcal{X} + \zeta_1^2(\mathcal{R} + \mathcal{W})\Big\},$$

$$\tilde{\Theta}_{31} = \begin{bmatrix} \mathcal{L}\mathcal{C} & 0 & 0 & 0 & 0 & 0 \\ \sqrt{\bar{\varphi}}\mathcal{G}\mathcal{L}\mathcal{C} & 0 & 0 & 0 & 0 & 0 \end{bmatrix}, \tilde{\Theta}_{33} = diag\{-I,\ -\mathcal{L}\}.$$

Then, the controller gain is derived by $\mathcal{K} = \mathcal{N}\mathcal{L}^{-1}$.

Proof . Define $\tilde{\mathcal{Q}} = \mathcal{X}\mathcal{Q}\mathcal{X}, \mathcal{K}\mathcal{L} = \mathcal{N}, \mathcal{X} = \mathcal{P}^{-1}, \tilde{\mathcal{W}} = \mathcal{X}\mathcal{W}\mathcal{X} > 0, \tilde{\mathcal{R}} = \mathcal{X}\mathcal{R}\mathcal{X}, \tilde{\mathcal{U}} = \mathcal{X}\mathcal{U}\mathcal{X}$, appropriate dimension matrix $\mathcal{L} = \mathcal{P}_2^{-1}, \tilde{\phi} = \mathcal{L}\phi\mathcal{L}$.

Using pre- and post-multiplying (15) with H_1 and pre- and post-multiplying (16) with H_2, one can see that (25) and (27) hold, where $H_1 = \text{diag}\{\mathcal{X}, \mathcal{X}\}$, $H_2 = \text{diag}\{\mathcal{X}, \mathcal{X}, \mathcal{X}, \mathcal{L}, I, \mathcal{L}, (\mathcal{R}+\mathcal{W})^{-1}, (\mathcal{R}+\mathcal{W})^{-1}\}$.

$$\Xi = \begin{bmatrix} \Theta_{11} & * & * \\ \Theta_{21} & \Theta_{22} & * \\ \Theta_{31} & 0 & \Theta_{33} \end{bmatrix} < 0, \tag{27}$$

where

$$\Theta_{11} = \begin{bmatrix} \Xi_{11} & * & * & * & * & * \\ \Xi_{21} & \Xi_{22} & * & * & * & * \\ \tilde{\mathcal{U}} & \tilde{\mathcal{R}} - \tilde{\mathcal{U}} & -\tilde{\mathcal{Q}} - \tilde{\mathcal{R}} & * & * & * \\ (1-\bar{\varphi})\mathcal{L}\mathcal{K}^T\mathcal{B}^T & -\alpha\mathcal{L}\phi\mathcal{C}\mathcal{X} & 0 & -\tilde{\phi} + \alpha\tilde{\phi} & * & * \\ \Xi_{51} & 0 & 0 & 0 & -\gamma^2 I & * \\ -\bar{\varphi}\mathcal{L}\mathcal{K}^T\mathcal{B}^T & 0 & 0 & 0 & 0 & -\bar{\varphi}\mathcal{L} \end{bmatrix},$$

$$\Xi_{11} = \mathcal{X}\mathcal{A}^T + \mathcal{A}\mathcal{X} + \tilde{\mathcal{Q}} - \tilde{\mathcal{R}} - \frac{\pi^2}{4}\tilde{\mathcal{W}},$$

$$\Xi_{21} = (\bar{\varphi} - 1)\mathcal{X}\mathcal{C}^T\mathcal{K}^T\mathcal{B}^T + \tilde{\mathcal{R}} - \tilde{\mathcal{U}} + \frac{\pi^2}{4}\tilde{\mathcal{W}},$$

$$\Xi_{22} = -2\tilde{\mathcal{R}} + \tilde{\mathcal{U}} + \tilde{\mathcal{U}}^T - \frac{\pi^2}{4}\tilde{\mathcal{W}} + \alpha\mathcal{X}\mathcal{C}^T\phi\mathcal{C}\mathcal{X}, \Xi_{51} = \mathcal{F}^T,$$

$$\Theta_{21} = \begin{bmatrix} \bar{\lambda}\mathcal{A}\mathcal{X} & -\bar{\lambda}(1-\bar{\varphi})\mathcal{B}\mathcal{K}\mathcal{C}\mathcal{X} & 0 & \bar{\lambda}(1-\bar{\varphi})\mathcal{B}\mathcal{K}\mathcal{L} & \bar{\lambda}\mathcal{F} & -\bar{\lambda}\bar{\varphi}\mathcal{B}\mathcal{K}\mathcal{L} \\ 0 & -\bar{\lambda}\rho\mathcal{B}\mathcal{K}\mathcal{C}\mathcal{X} & 0 & \bar{\lambda}\rho\mathcal{B}\mathcal{K}\mathcal{L} & 0 & \bar{\lambda}\rho\mathcal{B}\mathcal{K}\mathcal{L} \end{bmatrix},$$

$$\Theta_{22} = \text{diag}\left\{-(\mathcal{R}+\mathcal{W})^{-1} \quad -(\mathcal{R}+\mathcal{W})^{-1}\right\}, \Theta_{31} = \begin{bmatrix} \mathcal{C}\mathcal{X} & 0 & 0 & 0 & 0 & 0 \\ \sqrt{\bar{\varphi}}\mathcal{G}\mathcal{C}\mathcal{X} & 0 & 0 & 0 & 0 & 0 \end{bmatrix},$$

$$\Theta_{33} = \text{diag}\{-I, \ -\mathcal{L}\}.$$

Noting that $(\zeta\mathcal{R} - \mathcal{P})\mathcal{R}^{-1}(\zeta\mathcal{R} - \mathcal{P}) \geq 0, \zeta > 0$, it is easy to see that $-\mathcal{P}\mathcal{R}^{-1}\mathcal{P} \leq \zeta^2\mathcal{R} - 2\zeta\mathcal{P}$. Define $H_3 = \text{diag}\{I, I, I, I, I, I, P, P, I, I\}$ and $H_4 = \text{diag}\{I, I, I, I, I, I, X, X, I, I\}$. By using $\mathcal{C}\mathcal{X}$ and $\mathcal{N}$ instead of $\mathcal{L}\mathcal{C}$ and $\mathcal{K}\mathcal{L}$, and pre- and post-multiplying (27) with H_3 and H_4, respectively, one can obtain that the inequality (26) holds. This ends the proof. □

To solve the problem of equality (24) in Theorem 2, we use the optimization algorithm in [32], which can be expressed as

$$\begin{cases} \begin{bmatrix} -\kappa I & (\mathcal{L}\mathcal{C} - \mathcal{C}\mathcal{X})^T \\ (\mathcal{L}\mathcal{C} - \mathcal{C}\mathcal{X}) & -I \end{bmatrix} < 0, \\ \kappa \to 0, \end{cases} \tag{28}$$

where $\kappa > 0$ is a small enough constant. Furthermore, the controller gain could be calculated by (25), (26) and (28).

4. Simulation Examples

An application example of LFC systems in [33,34] is given to verify the efficacy of the method, whose nominal values are listed in Table 2.

Table 2. System parameters utilized in simulintion section.

Physical Quantity	$\mathcal{M}$**(kg·m²)**	$\mathcal{J}$**(Hz p.u. MW^{-1})**	$\mathcal{T}_g$**(s)**	$\mathcal{T}_{ch}$**(s)**	μ	$\mathcal{E}$
Values	0.1667	2.4	0.08	0.3	0.425	0.0083

Select the attack function $\eth(t) = -\tanh(\mathcal{G}y(t))$ [2] and $\mathcal{G} = \mathrm{diag}\{0.8,\ 0.1\}$. The mathematic expectation of the deception attack is given as $\bar{\varphi} = 0.5$. The disturbance is chosen as

$$\omega(t) = \begin{cases} 0.5\cos(0.1t), & 15 \le t \le 20 \\ 0, & \text{otherwise.} \end{cases}$$

Next, two cases are utilized to manifest the proposed method for LFC systems.

Case 1: The impact of deception attacks is not considered in the controller design in this case. Give the parameters $\zeta_0 = \zeta_1 = 0.01, \kappa = 0.1$. Choose the adaptive law parameters $\alpha = 0.8$, $\iota = 80$, sampling period $h = 0.05$, the upper bound of network-induced delay $\bar{\lambda} = 0.001$, and H_∞ performance index $\gamma = 15$. Then, the controller gain and weighting matrix can be figured out by Theorem 2 as follows

$$\mathcal{K} = \begin{bmatrix} 0.0627 & 0.2561 \end{bmatrix}, \phi = \begin{bmatrix} 0.3654 & 0.4298 \\ 0.4298 & 2.1692 \end{bmatrix}.$$

It is assumed that the initial condition of system is $x(0) = [-1.5 \ \ -1 \ \ 0.2 \ \ 0]^T$. The results are obtained in Figures 2–5. The state responses of the LFC system in Case 1 are shown in Figure 2, which indicates that the LFC system is stable after 60 s. Figure 3 illustrates the responses of control input. The adaptive law $\sigma(t)$ is shown in Figure 4, where the curve finally converges to the upper bound $\alpha = 0.8$, which indicates that the amount of transmitted signals is greatly reduced when the system is stable. Figure 5 illustrates the deception attack signals of simulation.

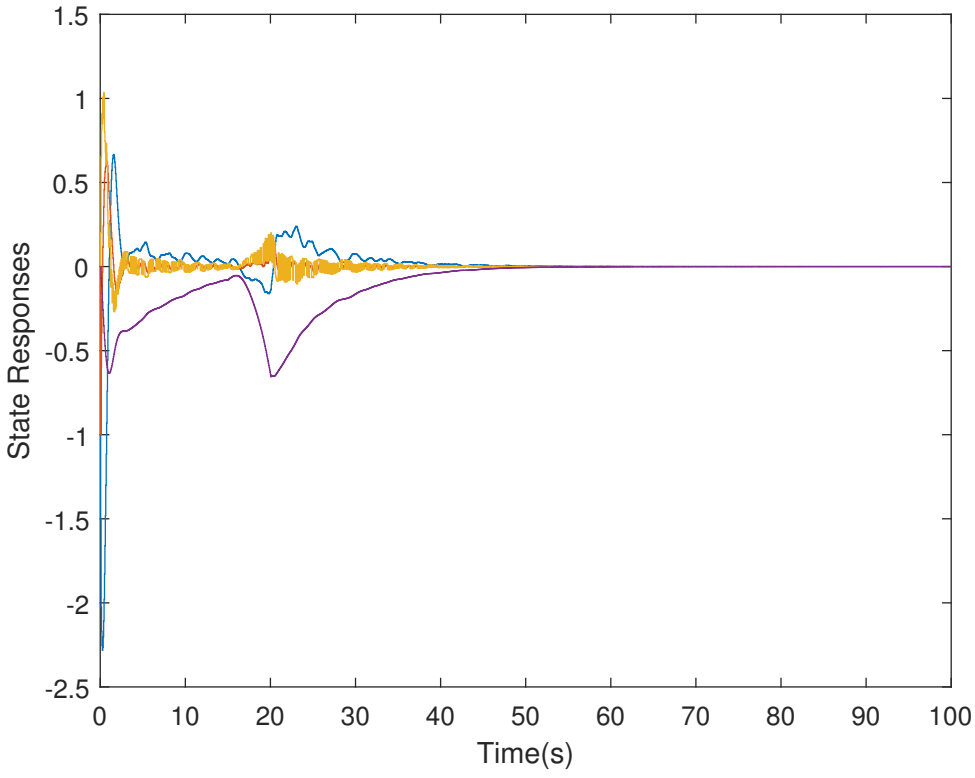

Figure 2. State responses of the LFC system in Case 1.

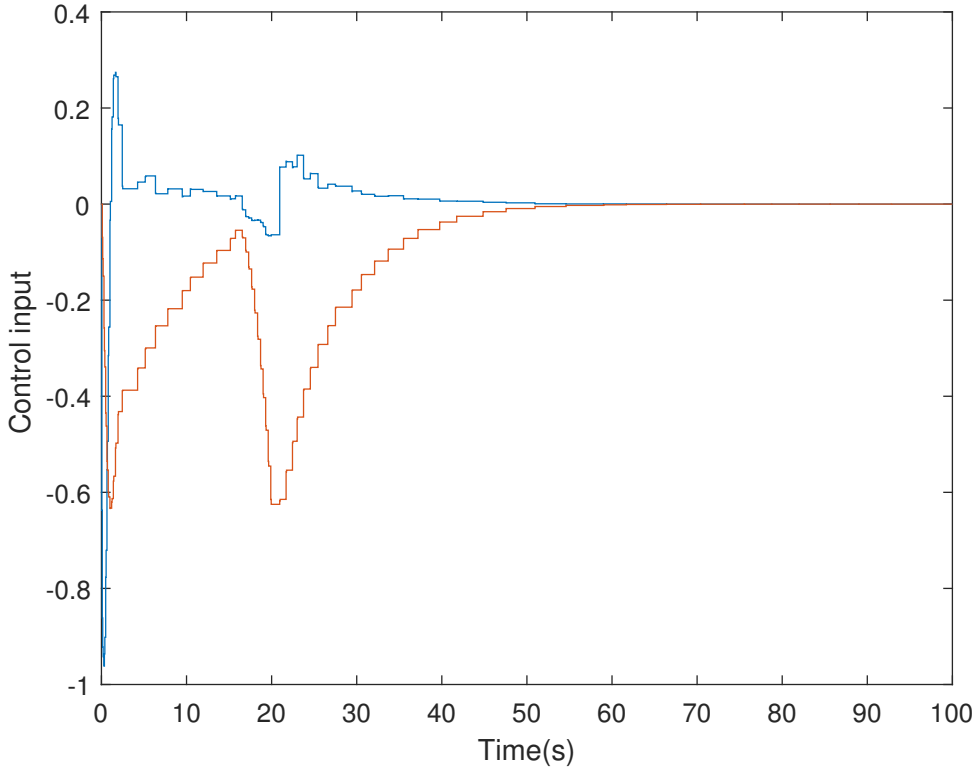

Figure 3. Control input of LFC systems in Case 1.

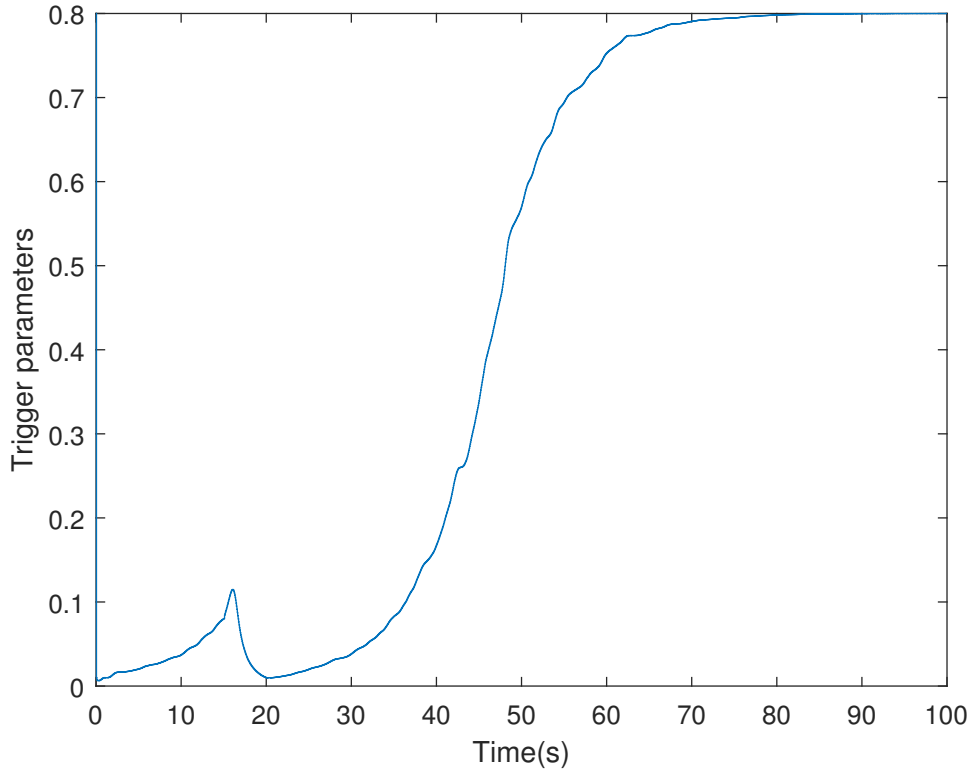

Figure 4. The threshold $\sigma(t)$ of the LFC system with the adaptive ETS in Case 1.

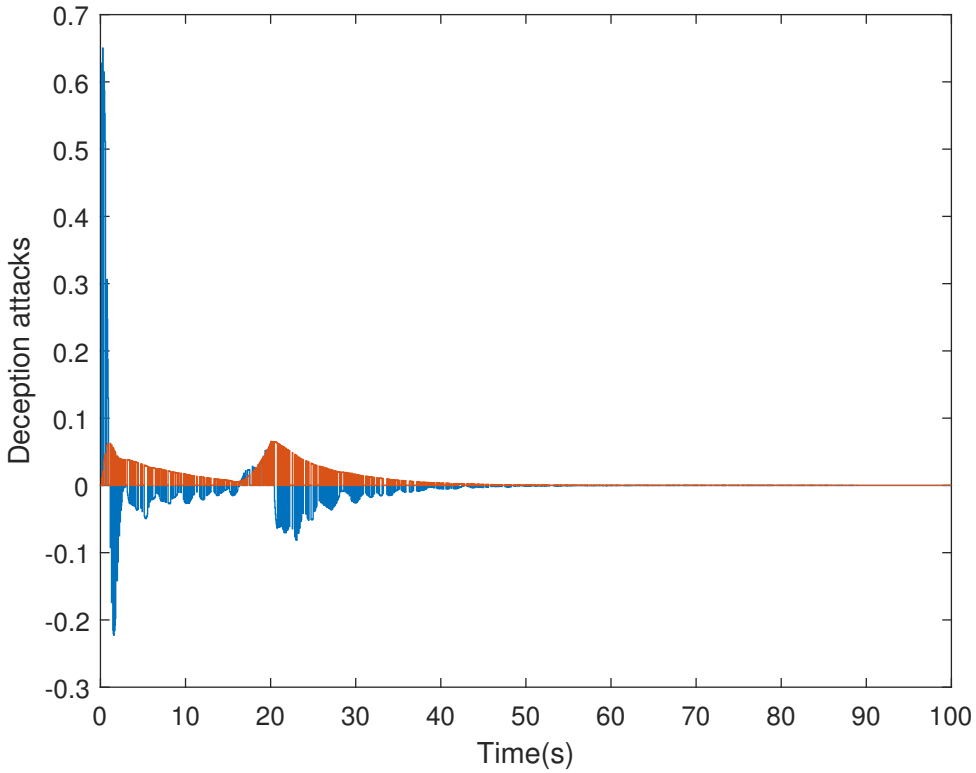

Figure 5. Deception attacks with $\bar{\varphi} = 0.5$.

Case 2: The impact of deception attacks in the design process of the controller is considered, and the mathematic expectation of the deception attack is given as $\bar{\varphi} = 0.5$. The other parameters are the same as those in Case 1. Then, we can obtain the controller gain and weighting matrix by Theorem 2 as follows

$$\mathcal{K} = \begin{bmatrix} 0.0374 & 0.5270 \end{bmatrix}, \phi = \begin{bmatrix} 0.2762 & 0.3004 \\ 0.3004 & 4.3447 \end{bmatrix}.$$

The simulated results of Case 2 are shown in Figures 6–8. Figure 6 depicts the system state trajectories, from which one can see that the state response curves of the turbine output power $\Delta\mathcal{H}_m$ and frequency deviation Δa of the closed-loop system subjected to changes in load demand. Compared to Figure 2 in Case 1, the turbine output power $\Delta\mathcal{H}_m$ and the system frequency deviation Δa approach zero in a shorter time, which indicates the use of controller in Case 2 can better mitigate the impact of deception attacks and suppress the fluctuations in system frequency and restore the stability of the system. The control input of the LFC system based on adaptive ETS are displayed in Figure 7.

Figure 8 exhibits the threshold $\sigma(t)$ of the system with adaptive ETS, where the triggering threshold is automatically adjusted even if the system suffers from the disturbance. When the system is stable, the adaptive threshold converges to a constant.

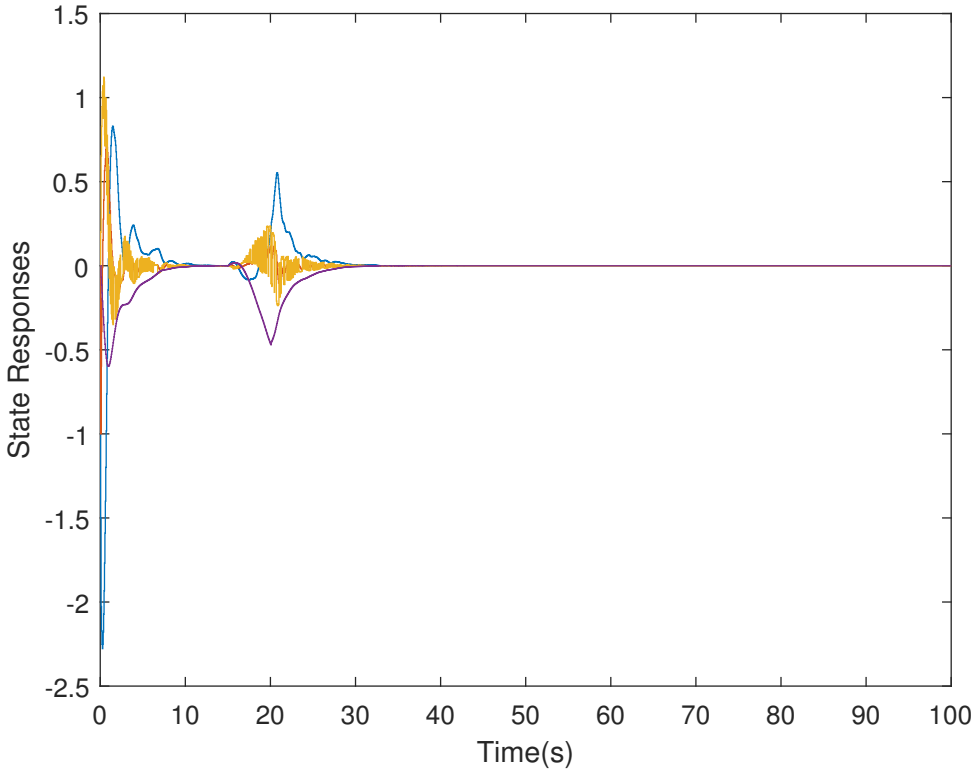

Figure 6. State responses of the LFC system based on the adaptive ETS in Case 2.

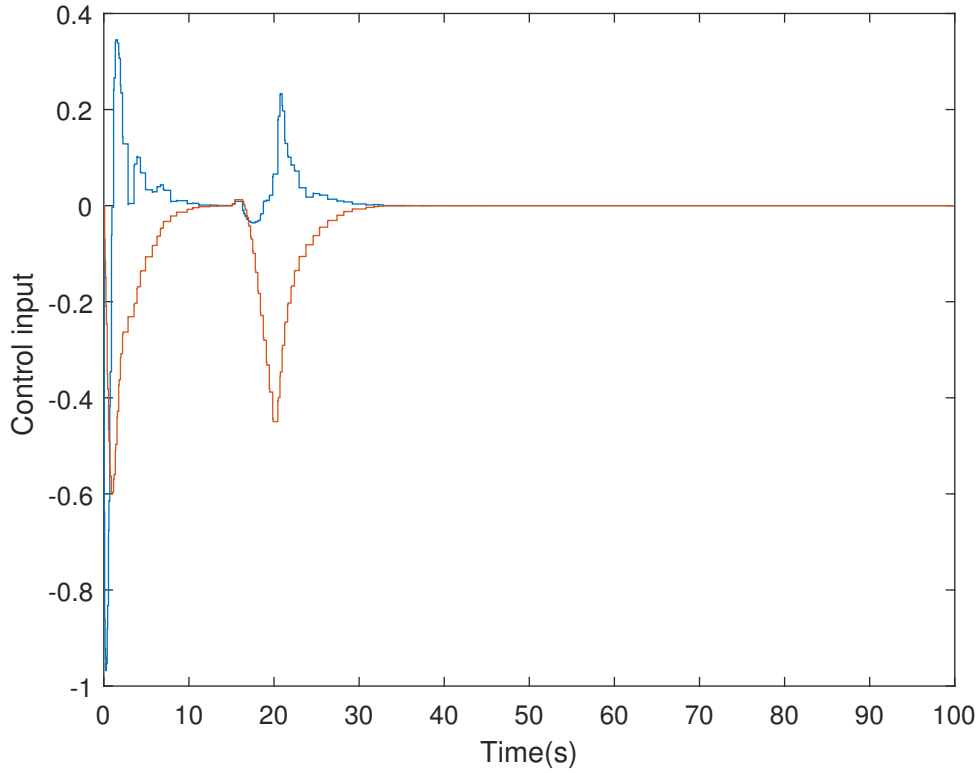

Figure 7. Control input of the LFC system based on the adaptive ETS in Case 2.

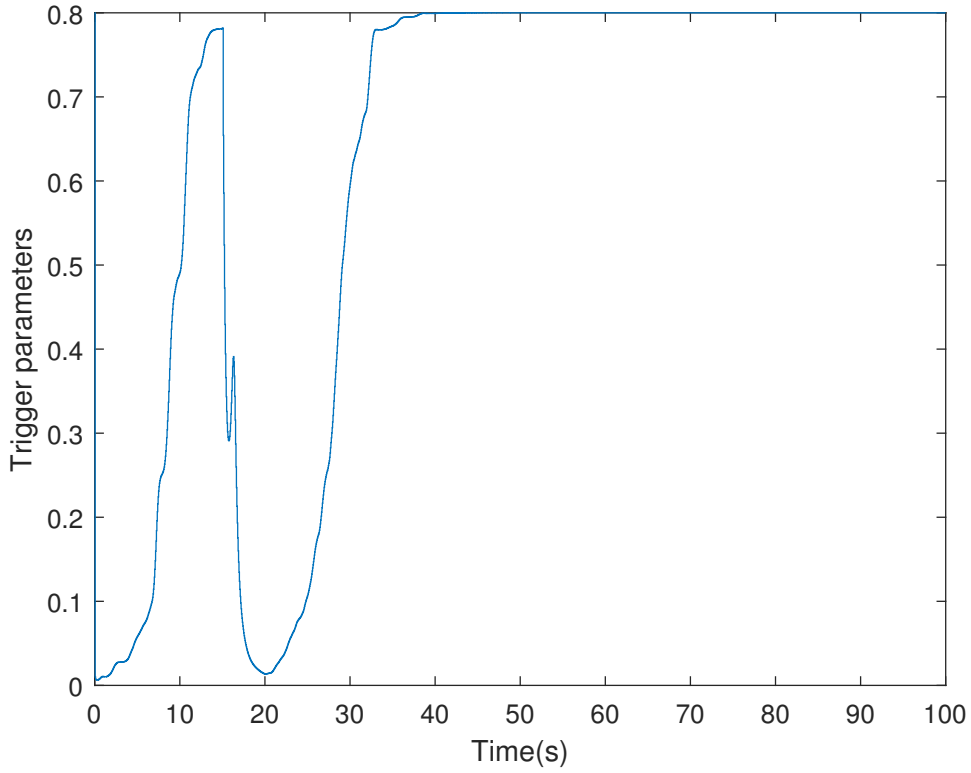

Figure 8. The threshold $\sigma(t)$ of the system with the adaptive ETS in Case 2.

To reflect the merits of the proposed method in saving the network bandwidth, we compare the adaptive ETS with the conventional ETS as follows:

(i) Consider $\sigma(t)$ in adaptive ETS (6) with the parameters $\alpha = 0.8, \iota = 1$.

(ii) The ETS in (6) with a fixed threshold $\bar{\sigma}$ is considered, which is reduced to a conventional ETS. Without loss of generality, the threshold is selected to be an average value that can be calculated by

$$\bar{\sigma} = \frac{\sum_{\nu=0}^{NDS} \sigma_\nu}{NDS}, \tag{29}$$

where $\nu \in N$, σ_ν denotes the ν-th the triggering threshold in adaptive ETS (6) at the ν-th sampling instant, and NDS is the number of data samplings.

Using LMIs, one can obtain the controller gains of two ETSs, which are listed in Table 3. The event-triggered constant $\bar{\sigma} = 0.7$ is calculated by (29) within 60 s.

Figures 9 and 10 plot the triggering and releasing intervals of the discussed system under two schemes, in which fewer sampling packets are released over the network under the adaptive ETS. For better analysis, the statistical results of the NDS, and the packet-releasing (NPR) and data-releasing rate (DRR) for two ETSs are written in Table 4, wherein $DRR = \frac{NPR}{NDS}$.

Table 3. Controller gains of two ETSs.

Schemes	Controller Gains $\mathcal{K}$
General ETS with fixed threshold ($\bar{\sigma} = 0.7$)	[0.0393 0.5584]
This work	[0.0374 0.5270]

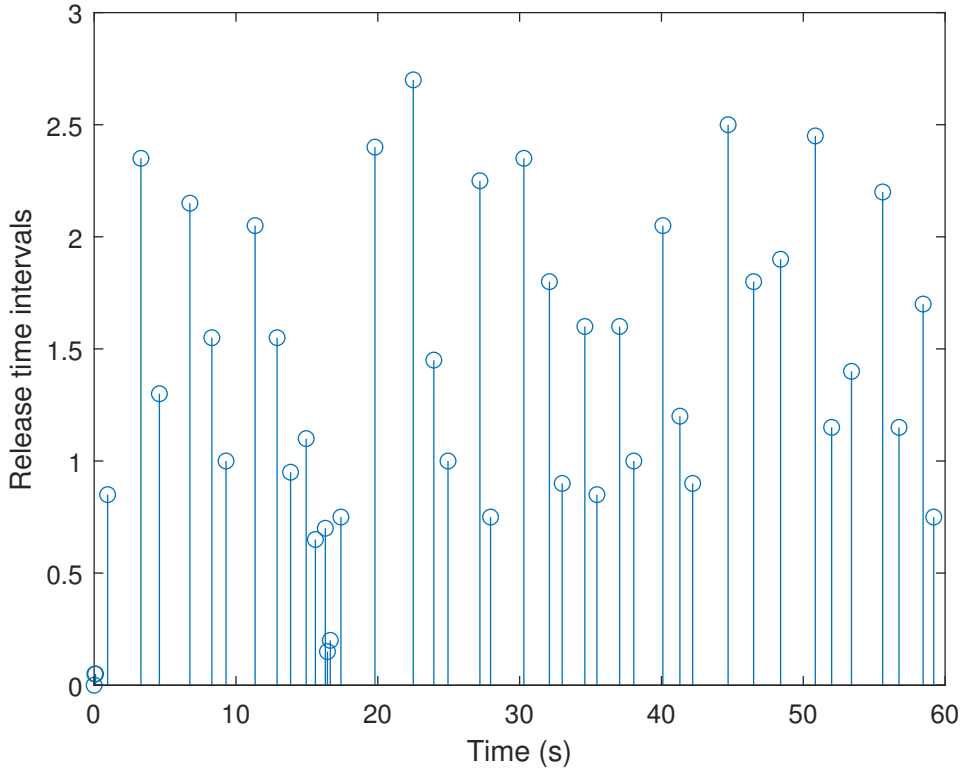

Figure 9. Release instants and release intervals with $\bar{\sigma} = 0.7$.

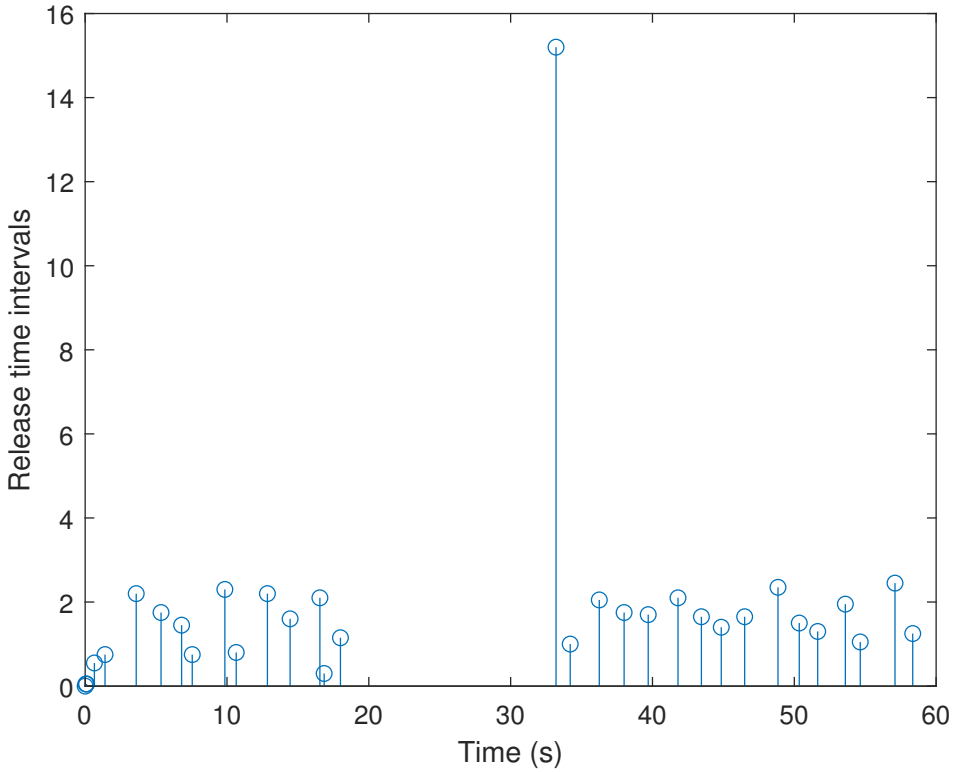

Figure 10. Release instants and release intervals with the adaptive ETS.

As shown in Table 4, the number of sampling data is 1200 within 60 s. Under the adaptive ETS (6) proposed in this paper, the number of released packets is 31, and the DRR is 2.58%. Compared to the DRR = 3.58% of the conventional ETS, the proposed adaptive

ETS can significantly reduce the transmission of unnecessary packets. This indicates that more communication resources can be saved by utilizing our developed adaptive ETS.

Table 4. The number of packets transmitted in 60 s with sampling period $h = 0.05$.

Schemes	NDS	NPR	DRR
General ETS with fixed threshold ($\bar{\sigma} = 0.7$)	1200	43	3.58%
This work	1200	31	2.58%

5. Conclusions

The problem of H_∞ LFC has been addressed for LFC systems under deception attacks by applying the developed adaptive ETS in this paper. To solve the issues of limited communication resources and deception attacks, a new adaptive ETS has been proposed, by which the thresholds for event-triggered conditions could be adapted to the changes in the system state under deception attacks. Based on the adaptive ETS, the average data released are lower than under the conventional ETS, and the perfomance of LFC systems subject to deception attacks can be guaranteed. Finally, the simulation results demonstrate the reliability of our proposed scheme. In future research, actuator saturation for LFC systems under cyber attacks will be worth consideration under the proposed adaptive ETS.

Author Contributions: All of the authors contributed substantially to this work: Conceptualization, X.Z. and X.S.; Methodology, F.Y. and X.Z.; Software, X.Z. and X.S.; Formal Analysis, X.Z.; Investigation, F.Y. and X.S.; Resources, F.Y.; Data Curation, X.Z.; Writing-Original Draft Preparation, Review and Editing, X.Z., F.Y. and X.S.; Project Administration, F.Y.; Funding Acquisition, F.Y. and X.S. All authors have read and agreed to the published version of the manuscript.

Funding: This research is supported by National Natural Science Foundation of China Grant No. 52005266, No. 62103193 and Postgraduate Research & Practice Innovation Program of Jiangsu Province Grant No. KYCX20_0855.

Institutional Review Board Statement: Not applicable.

Informed Consent Statement: Not applicable.

Data Availability Statement: Not applicable.

Conflicts of Interest: The authors declare no conflict of interest.

References

1. Hossain, M.M.; Chen, P. Observer-based event triggering H_∞ LFC for multi-area power systems under DoS attacks. *Inf. Sci.* **2021**, *543*, 437–453. [CrossRef]
2. Liu, J.; Gu, Y.; Zha, L.; Liu, Y.; Cao, J. Event-triggered H_∞ load frequency control for multiarea power systems under hybrid cyber attacks. *IEEE Trans. Syst. Man Cybern. Syst.* **2019**, *49*, 1665–1678. [CrossRef]
3. Zhang, C.K.; Jiang, L.; Wu, Q.; He, Y.; Wu, M. Delay-dependent robust load frequency control for time delay power systems. *IEEE Trans. Power Syst.* **2013**, *28*, 2192–2201. [CrossRef]
4. Pappachen, A.; Fathima, A.P. Critical research areas on load frequency control issues in a deregulated power system: A state-of-the-art-of-review. *Renew. Sustain. Energy Rev.* **2017**, *72*, 163–177. [CrossRef]
5. Tang, Y.; He, H.; Wen, J.; Liu, J. Power system stability control for a wind farm based on adaptive dynamic programming. *IEEE Trans. Smart Grid.* **2017**, *6*, 166–177. [CrossRef]
6. Chang, C.; Fu, W. Area load frequency control using fuzzy gain scheduling of PI controllers. *Electr. Power Syst. Res.* **1997**, *42*, 145–152. [CrossRef]
7. Liao, K.; Xu, Y. A robust load frequency control scheme for power systems based on second-order sliding mode and extended disturbance observer. *IEEE Trans. Ind. Inf.* **2017**, *14*, 3076–3086. [CrossRef]
8. Liu, F.; Li, Y.; Cao, Y.; She, J.; Wu, M. A two-layer active disturbance rejection controller design for load frequency control of interconnected power system. *IEEE Trans. Power Syst.* **2015**, *31*, 3320–3321. [CrossRef]
9. Liu, X.; Su, X.; Yang, R. Event-triggered sliding-mode control for multi-area power systems. *IEEE Trans. Ind. Electron.* **2017**, *64*, 6732–6741.
10. Wen, S.; Yu, X.; Zeng, Z.; Wang, J. Event-triggering load frequency control for multiarea power systems with communication delays. *IEEE Trans. Ind. Electron.* **2016**, *63*, 1308–1317. [CrossRef]

11. Liu, S.; Liu, P.X. Distributed model-based control and scheduling for load frequency regulation of smart grids over limited bandwidth networks. *IEEE Trans. Ind. Inf.* **2017**, *14*, 1814–1823. [CrossRef]
12. Basomingera, R.; Choi, Y.J. Learning from routing information for detecting routing misbehavior in ad hoc networks. *Sensors* **2020**, *20*, 6275. [CrossRef]
13. Gu, Z.; Park, J.H.; Yue, D.; Wu, Z.G.; Xie, X.P. Event-triggered security output feedback control for networked interconnected systems subject to cyber-attacks. *IEEE Trans. Syst. Man Cybern. Syst.* **2020**. [CrossRef]
14. Peng, C.; Yue, D.; Tian, E.; Gu, Z. Observer-based fault detection for networked control systems with network quality of services. *Appl. Math. Modell.* **2010**, *34*, 1653–1661. [CrossRef]
15. Junior, L.; Cristino, W.; Moraes, D.; Coreixas, C. A triggering mechanism for cyber-attacks in naval sensors and systems. *Sensors* **2021**, *21*, 3195. [CrossRef]
16. Fantacci, R.; Nizzi, F.; Pecorella, T.; Pierucci, L.; Roveri, M. False data detection for fog and internet of things networks. *Sensors* **2019**, *19*, 4235. [CrossRef]
17. Yan, S.; Gu, Z.; Park, J.H. Memory-event-triggered H_∞ load frequency control of multi-area power systems with cyber-attacks and communication delays. *IEEE Trans. Netw. Sci. Eng.* **2021**, *8*, 1571–1583. [CrossRef]
18. Gu, Z.; Sun, X.; Lam, H.K.; Yue, D.; Xie, X. Event-based secure control of T–S fuzzy based 5-DOF active semi-vehicle suspension systems subject to DoS attacks. *IEEE Trans. Fuzzy Syst.* **2021**. [CrossRef]
19. Peng, C.; Li, J.; Fei, M. Resilient event-triggering H_∞ load frequency control for multi-area power systems with energy-limited DoS attacks. *IEEE Trans. Power Syst.* **2017**, *32*, 4110–4118. [CrossRef]
20. Yue, D.; Tian, E.; Han, Q.L. A delay system method for designing event-triggered controllers of networked control systems. *IEEE Trans. Autom. Control.* **2013**, *58*, 475–481. [CrossRef]
21. Gu, Z.; Yue, D.; Tian, E. On designing of an adaptive event-triggered communication scheme for nonlinear networked interconnected control systems. *Inf. Sci.* **2018**, *422*, 257–270. [CrossRef]
22. Yan, S.; Gu, Z.; Nguang, S.K. Memory-event-triggered H_∞ output control of neural networks with mixed delays. *IEEE Trans. Neural Netw. Learn. Syst.* **2021**. [CrossRef]
23. Zhang, C.; Feng, G.; Qiu, J.; Shen, Y. Control synthesis for a class of linear network-based systems with communication constraints. *IEEE Trans. Ind. Electron.* **2013**, *60*, 3339–3348. [CrossRef]
24. Bemani, A.; Björsell, N. Distributed event triggering algorithm for multi-agent system over a packet dropping network. *Sensors* **2021**, *21*, 4835. [CrossRef]
25. Hu, S.; Yue, D.; Yin, X.; Xie, X.; Ma, Y. Adaptive event-triggered control for nonlinear discrete-time systems. *Int. J. Robust Nonlinear Control.* **2016**, *26*, 4104–4125. [CrossRef]
26. Yan, S.; Shen, M.; Nguang, S.K.; Zhang, G. Event-triggered H_∞ control of networked control systems with distributed transmission delay. *IEEE Trans. Autom. Control.* **2019**, *65*, 4295–4301. [CrossRef]
27. Liu, Y.; Chen, Y.; Li, M. Dynamic event-based model predictive load frequency control for power systems under cyber attacks. *IEEE Trans. Smart Grid.* **2020**, *12*, 715–725. [CrossRef]
28. Gu, Z.; Shi, P.; Yue, D.; Yan, S.; Xie, X. Memory-based continuous event-triggered control for networked T–S fuzzy systems against cyber-attacks. *IEEE Trans. Fuzzy Syst.* **2020**, *29*, 3118–3129 [CrossRef]
29. Gu, Z.; Shi, P.; Yue, D.; Ding, Z. Decentralized adaptive event-triggered H_∞ filtering for a class of networked nonlinear interconnected system. *IEEE Trans. Cybern.* **2018**, *49*, 1570–1579. [CrossRef]
30. Gu, Z.; Shi, P.; Yue, D. An adaptive event-triggering scheme for networked interconnected control system with stochastic uncertainty. *Int. J. Robust Nonlinear Control.* **2017**, *27*, 236–251. [CrossRef]
31. Peng, C.; Zhang, J.; Yan, H. Adaptive event-triggering H_∞ load frequency control for network-based power systems. *IEEE Trans. Ind. Electron.* **2017**, *65*, 1685–1694. [CrossRef]
32. Gu, Z.; Fei, S.M.; Zhao, Y.Q.; Tian, E.G. Robust control of automotive active seat-suspension system subject to actuator saturation. *J. Dyn. Syst. Meas. Control.* **2014**, *136*, 041022. [CrossRef]
33. Pham, T.N.; Nahavandi, S.; Trinh, H. Static output feedback frequency stabilization of time-delay power systems with coordinated electric vehicles state of charge control. *IEEE Trans. Power Syst.* **2016**, *32*, 3862–3874. [CrossRef]
34. Tian, E.; Peng, C. Memory-based event-triggering H_∞ load frequency control for power systems under deception attacks. *IEEE Trans. Cybern.* **2020**, *50*, 4610–4618. [CrossRef]